The Physics of Neoclassical Tearing Modes and Their Stabilisation by ECCD in ASDEX Upgrade

[1]H. Zohm, [2]G. Gantenbein,[1]A. Gude, [1]S. Günter, [1]F. Leuterer, [1]M. Maraschek,
[2]J. Meskat, [1]W. Suttrop, [1]Q. Yu, [1]ASDEX Upgrade Team, [1]ECRH-Group (AUG)

[1] MPI für Plasmaphysik, D-85748 Garching, Germany, EURATOM-Association
[2] Institut für Plasmaforschung, Pfaffenwaldring 31, D-70569 Stuttgart, Germany

e-mail contact of main author: zohm@ipp.mpg.de

Abstract The physics understanding of Neoclassical Tearing Modes (NTMs) gained through experiments and modelling at ASDEX Upgrade is presented. The onset β_N for NTM is found to be proportional to the normalised ion gyroradius ρ^* and independent of the normalised collisionality ν^* for a wide range of ν^*. This scaling is in accordance with both polarisation current and $\chi_\perp/\chi_\parallel$ model, if for the latter, the heat flux limit on parallel heat conductivity is taken into account. Analysis of the structure and dynamics of NTMs validates the negative Δ'. Complete stabilisation using ECCD has been demonstrated at $\beta_N = 2.5$ and with about 10 % of the total heating power. The results are in good qualitative agreement with modelling using the Rutherford equation and in quantitative agreement with a 2 dimensional nonlinear cylindrical tearing mode code. A precise positioning of the ECCD microwave beam, so far achieved by feed-forward variation of B_t, is required for efficient stabilisation.

1. Introduction

Neoclassical Tearing Modes (NTMs) in tokamaks lead to magnetic islands that limit the ratio of kinetic pressure p to the pressure associated with the magnetic field B, i.e. the value of $\beta = 2\mu_0\langle p\rangle/B^2$ which measures the efficiency of the magnetic confinement [1], [2]. The analysis of the β-limit due to NTMs as well as its possible extension by NTM stabilisation is therefore a key area of tokamak MHD research.

NTM physics is usually discussed in terms of the generalised Rutherford equation for the temporal evolution of the island width W, which takes into account the various destabilising and stabilising terms [2]:

$$\frac{\tau_s}{r_s}\frac{dW}{dt} = r_s\Delta'(W) + r_s\beta_p\Big(a_2\sqrt{\frac{r_s}{R_0}}\frac{L_q}{L_p}\frac{W}{W^2+W_0^2} - a_3\frac{r_s}{R_0^2}\frac{L_q^2}{L_p}\frac{1}{W}$$

$$- a_4 g(\nu)(\rho_p\frac{L_q}{L_p})^2\frac{1}{W^3}\Big) - a_5\frac{L_q r_s}{2\sqrt{\pi}}\frac{I_{ECCD}}{I_p(r_s)}f(W)\frac{1}{W^2} \tag{1}$$

Here, r_s is the radius of the resonant surface, β_p the poloidal β, $\tau_s = 1.22\mu_0\sigma r_s^2$ the resistive timescale (with σ being the electrical conductivity), R_0 the tokamak major radius and $L_p = p/\nabla p$ and $L_q = q/\nabla q$ are the pressure and shear length. The first term on the right hand side is the contribution of the equilibrium current profile, characterised by the instability parameter $\Delta' = (d\psi/dr|_{r_s^+} - d\psi/dr|_{r_s^-})/\psi$ with ψ being the perturbed flux function and r_s^+ and r_s^- denoting the outer and inner minor radius of the island separatrix at the O-point. The second term describes the bootstrap current drive where W_0 is the critical island width above which the pressure profile is no longer fully flattened [3], the third one describes the stabilising influence of the toroidal geometry [4], the fourth the stabilising polarisation current [5] (where $g(\nu)$ is a function

that changes from small to large values below a certain collisionality ν) and the last term is an externally added helical current, e.g. by ECCD [6]. The function $f(W)$ has the limiting values $f(W) = 1$ if the deposition width d of the ECRH is small compared to W and $f(W) = 0.3W/d$ for $d \gg W$ (i.e. only the fraction deposited within the island counts). In the following sections, we discuss our current understanding of NTM physics and our recent experimental results concerning stabilisation of NTMs by ECCD.

2. NTM physics

Understanding NTM physics is essential for predicting their occurrence and for developing adequate means for avoiding or stabilising these modes. In the following, we will discuss the physics understanding of NTMs gained at ASDEX Upgrade through experiment and modelling.

On ASDEX Upgrade, the critical nromalised beta, $\beta_N = \beta/(I_p/(aB))$ for NTM onset has been found to scale proportional to the normalised ion gyroradius ρ^* with a very weak dependence on the normalised collisionality ν^* [7]. The database supporting this conclusion has been broadened by including NTMs occurring during pellet fuelled discharges as well as by comparison to NTM data from the old ASDEX tokamak [8]. Fig. 1 shows a compilation of ASDEX Upgrade data.
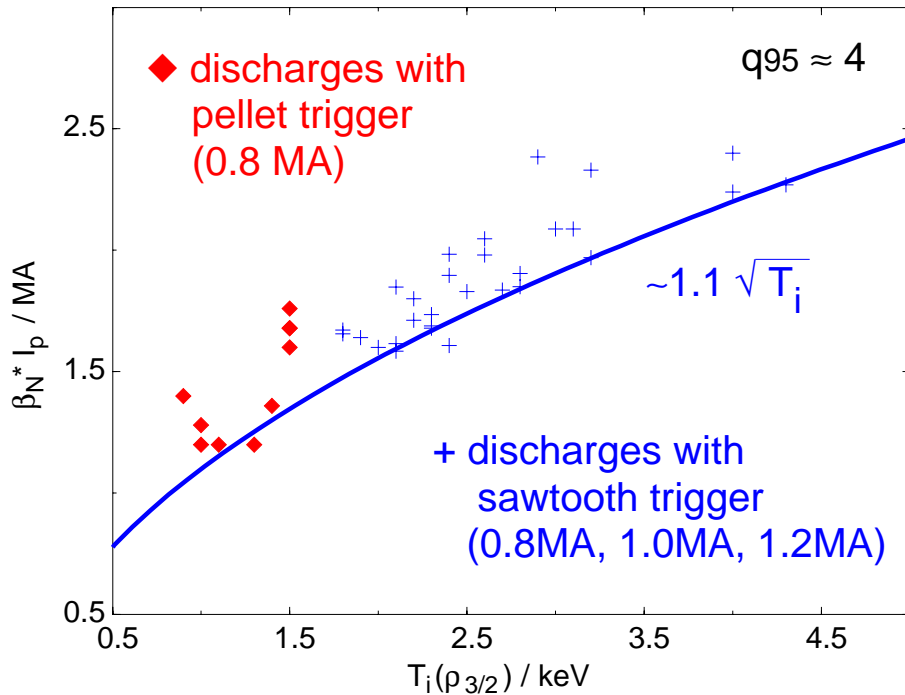

FIG. 1: *Onset* β_N *for NTMs in ASDEX Upgrade as function of* T_i*. The data points span a wide range in collisionality, but can be well described by a pure* ρ^**-scaling.*

Although the pellet points lie at substantially lower T_i and higher density and thus lead to a strong increase in ν^* (more than an order of magnitude variation is captured in Fig. 1), the $\sqrt{T_i}$ scaling is still valid. This linear ρ^*-scaling has recently also been found in JET [9]. However, in a density range approaching the Greenwald limit, NTMs can be suppressed by increasing ν^* [10]. The threshold collisionality was found to be well described by the expression given from the polarisation current model, i.e. $\nu_{ii}/(m\omega^*\varepsilon) > C$ with ω^* the electron diamagnetic drift frequency and $C \approx 0.03$. The weak ν^*-dependence once a threshold in ν^* is crossed is consistent with the abovementioned variation of the function $g(\nu)$ in Eqn. (1).

In ASDEX Upgrade, NTMs may occur in a sequence of modes that descends from close to $q = 1$ to a certain outermost surface determined by the local onset conditions (usually, the final mode is a (3,2) or, at lower densities, a (2,1) in ASDEX Upgrade). An important observation has been that NTMs of different helicities never coexist in a stationary state. A typical example is shown in Fig. 2, where a sequence of a (3,2) mode followed by a (2,1) is shown.
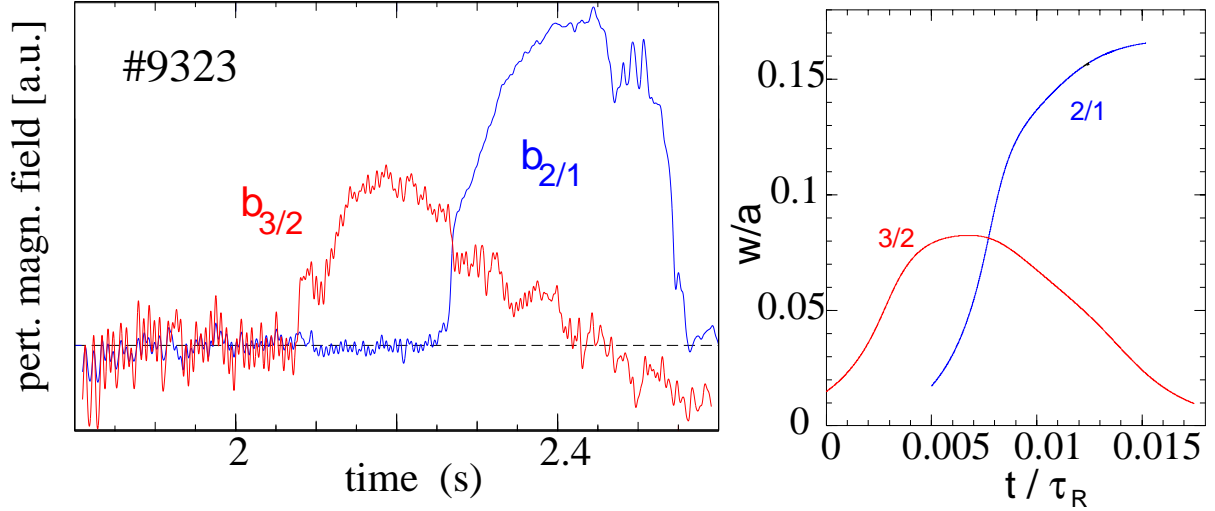

FIG. 2: *Temporal sequence of (3,2) and (2,1) NTMs in ASDEX Upgrade. After the (2,1) mode grows to sufficient level, the (3,2) mode vanishes. The sudden drop of the (2,1) signal at 2.5 s indicates a locked mode, i.e. the mode is still there, but not seen on the Mirnov coils. The experimental data are well reproduced by the modelling (right figure)*

This behaviour has been modelled using a nonlinear cylindrical tearing mode code [11]. The experimental observations can be explained by the nonlinear interaction between the tearing modes of different helicity: a nonresonant perturbation of sufficient magnitude tends to decrease the pressure perturbation at the resonant surface, thereby reducing the bootstrap drive for this particular mode. Thus, if a mode is more unstable than another one, it will reduce the drive of the less unstable mode and finally remove it. This is shown in the right part of Fig. 2. An interesting consequence of this theory is that it predicts that a non-resonant helical perturbation of sufficient size should be able to suppress NTMs [12].
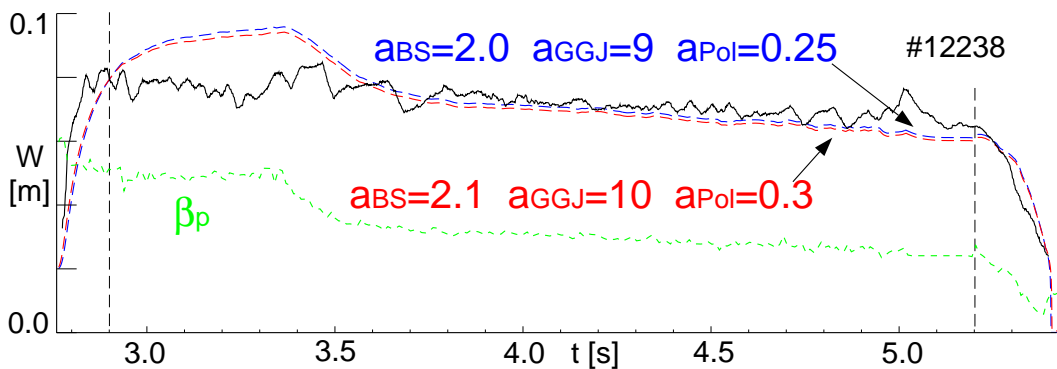

FIG. 3: *Modelling of the temporal evolution of a (3,2) NTM in ASDEX Upgrade. The experimental data are well reproduced with the coefficients $a_2 - a_4$ given in the figure.*

The temporal evolution of the NTM growth and decay has also been modelled using Eqn. (1). All input data are taken from the experiment as function of time, except Δ' which is set to $-m/r_s$,

in accordance with the theoretical expectation and the experimentally determined value (see below). Then, the parameters $a_2 - a_4$ are adjusted to provide a best fit to $W(t)$ for a number of discharges. A typical result is shown in Fig 3. It can be seen that for the parameters given in the figure, a good agreement is found. The fits shown are the best fit for this particular discharge as well as a best fit to four different discharges that are well described by this one set of parameters. Concerning the ambiguity in the determination of the parameters, it must be stated that several combinations providing reasonable fits exist. If W_0 is set to the small value predicted by classical parallel conductivity, it is impossible to determine a_2 and a_3 separately, since the W and β dependence of the terms is the same and the variation in other parameters is small. Setting W_0 to 1.8 cm (using the heat flux limit, see below), this problem is partly resolved. It should be noted that the ambiguity in a_4 also decreases when $W_0 = 1.8$ cm is introduced.

With ECE, we measure the local T_e with good temporal and spatial resolution. From this measurement, the isothermals can be reconstructed. These coincide with the flux surfaces, provided the parallel heat flux is much higher than the perpedicular one. This, however, is not the case near the island's X-points, where the field line gets very long. We have modelled the T_e-distribution across an island taking into account the finite ratio of $\chi_\perp$ to $\chi_\parallel$ as well as the realistic magnetic geometry (i.e. non-parabolic equilibrium flux and realistic assumption about the perturbed flux) [13]. This allows to approximately infer the perturbed flux function. Fig. 4 shows an example.
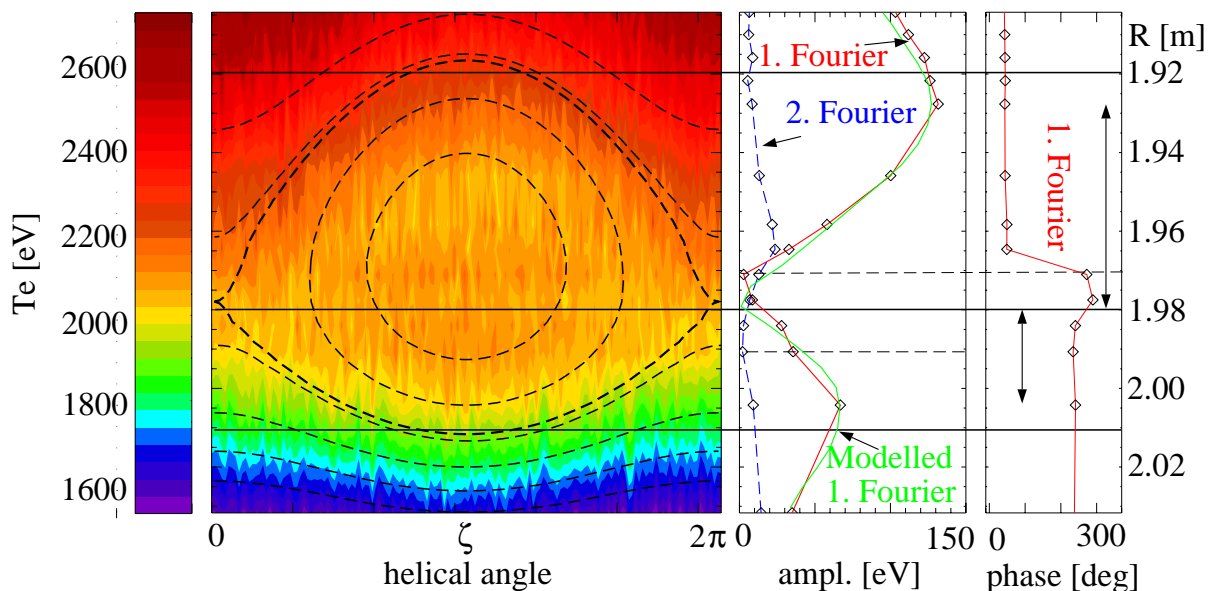

FIG. 4: *Measured T_e contours of a (3,2) NTM in ASDEX Upgrade. The right figures show the amplitude and the phase of the first and second Fourier component of the T_e-perturbation, from which island separatrix and r_s are inferred. A fit to the first Fourier component leading to the flux surfaces indicated in the left figure is shown, too.*

From the Fourier components of the perturbed T_e, we can infer the island width and the position of the resonant surface (indicated by horizontal lines). From the inferred perturbed flux, we can calculate the instability parameter Δ'. As expected for an NTM, Δ' is found to be negative and actually well matches the expected value of $\Delta' r_s \approx -m$ (for the example shown, $\Delta' r_s \approx -3.22$), but there are large error bars on the absolute value.

It has been pointed out that the finite ratio of $\chi_\perp/\chi_\parallel$ leads to a critical island size W_0, below which T_e across the island is not completely flattened, leading to a reduced bootstrap drive [3]. Usually, $\chi_\parallel$ is calculated using the classical Spitzer formula χ_{Sp}. However, for ASDEX Upgrade parameters, this is only valid in a region of roughly one millimeter around the island separatrix,

where the connection length L_c is indeed high enough to garantuee that many collisions take place along the gradient length. Well inside the island, a reduction ('heat flux limit') must be applied. Following [14], we use the form

$$\chi_\parallel = \frac{\chi_{Sp}}{\sqrt{1 + (3.16\frac{v_{th,e}}{\nu_{ei}L_c})^2}} \qquad (2)$$

where $v_{th,e}$ is the electron thermal velocity and ν_{ei} the electron-ion collision frequency. This means that throughout most of the island region, $\chi_\parallel$ is drastically reduced with respect to χ_{Sp}. As a consequence, W_0 now is of the order of 1.8 cm, whereas its value is 8 mm using the Spitzer formula. In addition, the scaling of W_0, which is proportional to $(\chi_\perp/\chi_\parallel)^{1/4}$ now changes: Assuming gyro-Bohm scaling for the perpendicular transport ($\chi_\perp \propto T^{3/2}/B^2$), we now find that the critical β_N scales like $\beta_N \propto \rho^*$ instead of $\beta_N \propto \rho^*\sqrt{\nu^*}$ using χ_{Sp}, provided that the spontaneously produced seed islands have constant width (a possible scaling of the spontaneous seed island size with magnetic Reynolds number is not taken into account). Thus, both scaling and absolute value of W_0 now agree with the experimental findings [7]. In particular, the ρ^*-scaling observed on ASDEX Upgrade is now in agreement with both the polarisation current and the $\chi_\perp/\chi_\parallel$-model, meaning that we cannot easily decide if one or the other (or both) are relevant in determining the onset value of β_N. The possible importance of the $\chi_\perp/\chi_\parallel$-term may, however, explain the observation that in ASDEX Upgrade, the critical seed island width required for NTM triggering seems to become smaller with increasing β_p [15].
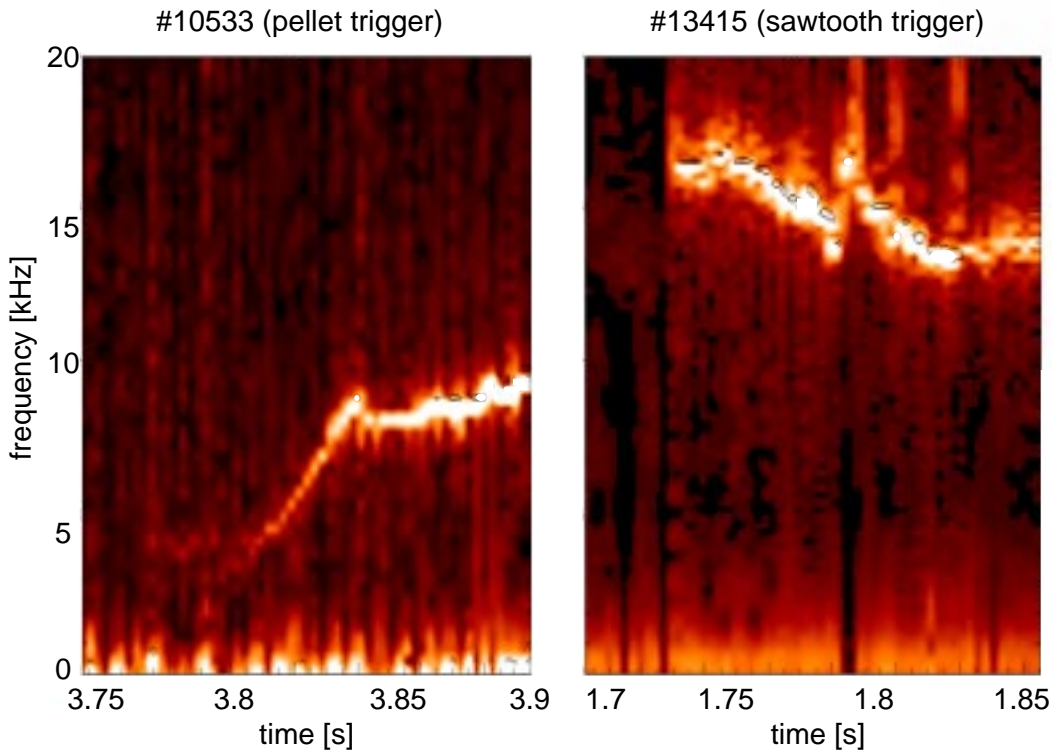

FIG. 5: *Temporal evolution of (3,2) NTM frequency during formation: a pellet triggered NTM comes from very low frequencies (left), whereas a usual (sawtooth triggered) NTM starts from a higher frequency (right).*

Usually, NTMs in ASDEX Upgrade are initiated by a sawtooth crash or, at higher β, by fishbones; in some cases, at even higher β, they may occur without noticeable external perturbation

[15]. In pellet fuelled discharges, we often observe that NTMs are triggered by the ablating pellet itself. Although the fact that higher densities, at constant β, lead to lower ρ^* can explain why the plasma becomes more vulnerable to NTMs (as seen in Fig. 1), the mechanism of seed island generation is not straightforward. A possible explanation is that, as the ablating pellet crosses the resonant surface, a closed flux tube with high density and low temperature develops that can lead to tearing, thus providing a seed island. This hypothesis is supported by the observation that a pellet triggered NTM starts to rotate from very low frequencies, which indicates that the seed island was generated by a perturbation with very low or zero rotation in the laboratory frame. In contrast, usual NTMs start at the rotation frequency of the $(1,1)$ mode connected to the sawtooth or slightly higher. This is shown in Fig. 5 for two cases with a $(3,2)$ mode. The difference in absolute value of $n = 2$ frequency is due to the lower beam power and higher density in the pellet triggered case ($v_{rot} \propto P_{NBI}/n$).

3. Stabilisation of NTMs by ECCD

Since NTMs set the β-limit in ASDEX Upgrade discharges with positive shear, a method to remove or avoid them is of great importance. A successful demonstration of such a method is also very desirable in view of a next-step experiment such as ITER-FEAT. On ASDEX Upgrade, we carry out experiments to stabilise NTMs by ECRH and ECCD in lower single null diverted H-mode plasmas at 0.8 MA, $B_t = 2.1$ T (resulting in $q_{95} \approx 4$) at typical densities of $5 - 6 \times 10^{19}$ m^{-3}. At NBI heating powers of 7.5 - 10 MW, $(3,2)$ NTMs develop at $\beta_N \approx 2.5$. The stabilisation of $(2,1)$ NTMs, which occur at lower densities, has so far not been studied. This will be done in the next experimental campaign. We inject up to 1.2 MW of ECRH (140 GHz, 2nd harmonic X-mode absorption on the high field side) into the plasma. By changing the injection angle, we vary the amount of driven current. Feed-forward scans in B_t of 5-10 % within 1 s, i.e. slow compared to the island growth time, are used to fine-tune the radial position of the absorption location. This effectively provides a linear increase of current driven within the island. The experiments can either be done in modulate ('AC') mode (i.e. synchronised with the rotating island) or by continuous ('DC') injection. Previous experiments on the stabilisation of NTMs by ECRH/ECCD in ASDEX Upgrade have been reported in [16], [17]. The main results from these experiments can be summarised as follows:

• There is no significant difference between AC and DC stabilisation. This is due to the fact that the fast electrons generated by ECCD quickly equilibrate along the field lines so that power deposited with finite width near the X-point does not generate substantial current within the island.

• With a power level sufficient for complete stabilisation with co-ECCD, ctr-ECCD results in only small changes of the mode amplitude, suggesting a significant contribution of direct CD in the stabilisation process.

• At $\beta_N \approx 2.2 - 2.5$, a $(3,2)$ NTM can be completely stabilised by applying an ECCD power of about 10 % of the total heating power, corresponding to 15 - 20 kA of helical current driven within the island. With less power, a reduction of the mode amplitude is observed.

• The radial localisation of the absorption position has to be exact within ca. ± 2 cm in ASDEX Upgrade. In case the ECCD power is located further away from r_s, no effect is observed.

• In the experiments conducted so far, β does not recover its full value at mode onset, although the mode is completely stabilised. This is attributed to a confinement degradation during ECRH/ECCD in this scenario (see also [18]).

Extensive modelling of the NTM stabilisation by ECRH and ECCD has been done using a cylindrical nonlinear tearing mode code [19]. In particular, the modelling shows that the main stabil-
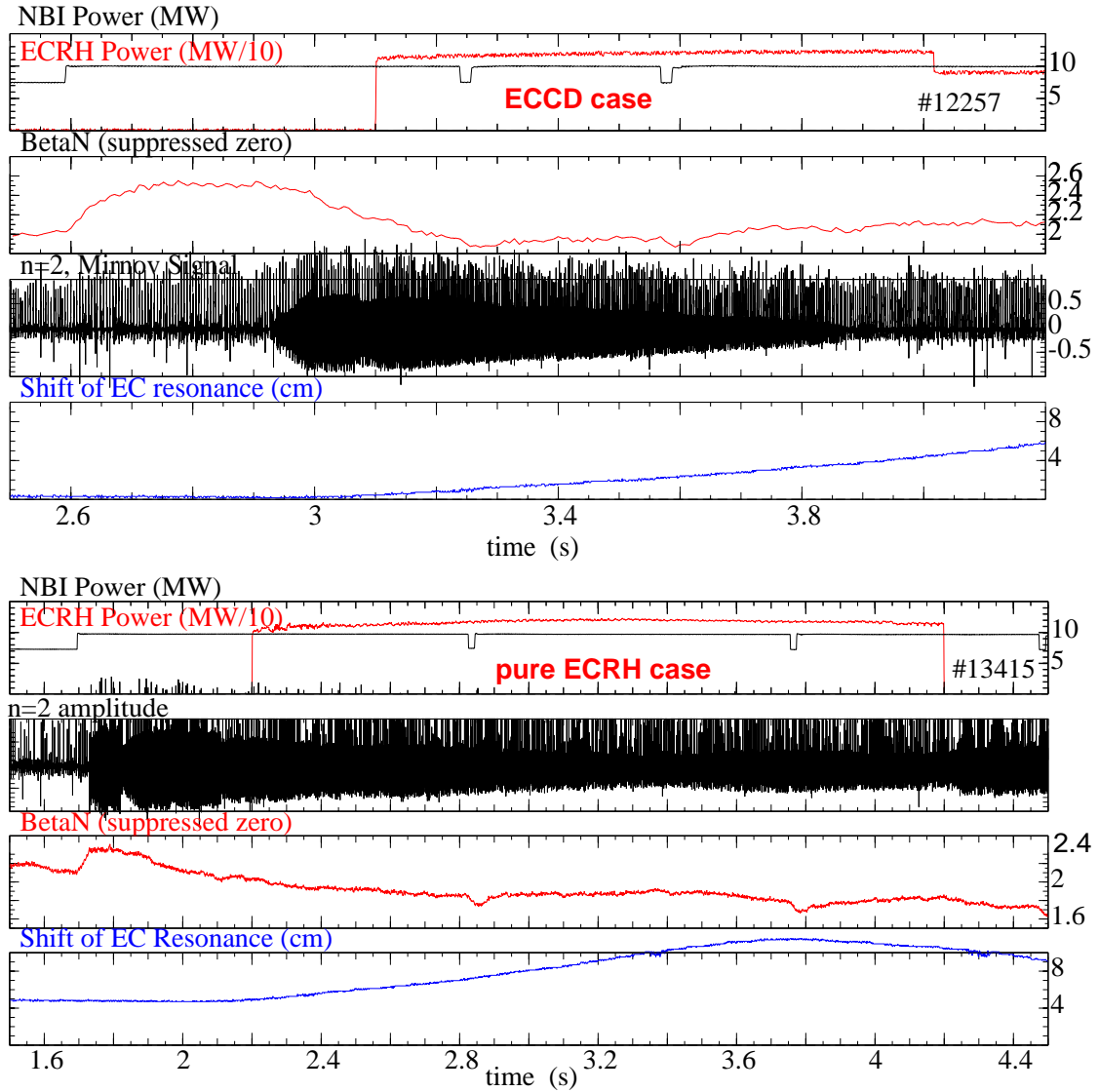
FIG. 6: *Comparison of NTM stabilisation experiments with ECCD (upper traces) and with pure ECRH (lower traces). For similar discharge parameters, the application of pure ECRH leads to only a small reduction of the NTM amplitude, whereas ECCD of the same power leads to complete stabilisation.*

ising effect comes from the direct generation of helical current within the island by ECCD. The related change in equilibrium current profile is smaller; the Δ'-variation can only account for roughly 10-20 % of the stabilising effect [17].

To verify the small contribution of island heating mentioned above, we carried out experiments using pure ECRH. A comparison between an ECRH and an ECCD discharge is shown in Fig. 6. In these experiments, B_t was scanned over a large range to adjust for optimum location. In the ECRH case, this location is at the position where the mode amplitude exhibits a minimum during the scan. It was found that the optimum position is obtained at slightly higher B_t than in the ECCD case. This can be explained by the Doppler shifted absorption maximum in the case of ECCD with respect to ECRH. The small effect in the case of pure ECRH at the power level of 1.2 MW, where ECCD completely stabilises the mode, directly verifies the importance of the current driven by ECCD that had previously been deduced from co/counter ECCD comparison. Code modelling shows that the small stabilising effect should mainly come from a helical current due to the increased conductivity within the island. However, the predicted change in T_e within

the island is of the order of 10-20 eV and very localised, so that we cannot verify it at present with our ECE measurements. Consistently, we find no significant local increase of T_e within the island during ECRH within the experimental resolution.

Our experiments show that the precise positioning is a necessary prerequisite for NTM control (the time interval of optimum stabilisation in the pure heating case in Fig. 6 translates to a region of approx. 4 cm). Thus, a feedback control of the radial position of the absorption is highly desirable. This will be one of the future aims of the ASDEX Upgrade experimental program.

4. Summary and conclusions

NTMs are the main β-limiting MHD event in conventional scenarios in ASDEX Upgrade. Their onset β_N scales proportional to ρ^* without significant ν^* dependence over a wide range of ν^*. This behaviour is consistent with the polarisation current model and, if the heat flux limit for parallel heat flow is taken into account, also with the $\chi_\perp/\chi_\parallel$-model. With about 10 % of the total heating power, a (3,2) NTM can be stabilised by ECCD, the main stabilising effect being the local helical current generated by ECCD. Pure ECRH is much less effective in stabilising the mode. Significant and flexible enhancement of β by this method will require feed-back controlled adjustment of the absorption location because the efficiency depends crucially on the exact positioning. The experimental results are in qualitative agreement with the generalised Rutherford equation and in quantitative agreement with a nonlinear cylindrical tearing mode code.

References

[1] CHANG, Z. et al., *Nucl. Fusion* **34** (1994) 1309.

[2] SAUTER, O. et al., *Phys. Plasmas* (1997).

[3] FITZPATRICK, R., *Phys. Plasmas* **2** (1996) 825.

[4] GLASSER, A. H. et al., *Phys. Fluids* **12** (1975) 875.

[5] WILSON, H. et al., *Phys. of Plasmas* **3** (1996) 248.

[6] ZOHM, H., *Phys. Plasmas* **4** (1997) 3433.

[7] GÜNTER, S. et al., *Nucl. Fusion* **38** (1998) 1431.

[8] MARASCHEK, M. et al., *Controlled Fusion and Plasma Physics, Proceedings of the 27th Conference, Budapest* (2000) P3.047.

[9] BUTTERY, R. et al., *Controlled Fusion and Plasma Physics, Proceedings of the 27th Conference, Budapest, to appear in Plasma Phys. Contr. Fusion.* (2000),

[10] MARASCHEK, M. et al., *Plasma Phys. Contr. Fusion* **41** (1999) L1.

[11] YU, Q. et al., *Acc. by Nucl. Fusion* (2000).

[12] YU, Q. et al., *Acc. by Phys. Rev. Lett.* (2000).

[13] MESKAT, J. P. et al., *Controlled Fusion and Plasma Physics, Proceedings of the 26th Conference, Maastricht* (1999) P4.002.

[14] CHANG, Z. et al., *Phys. Fluids B* **4** (1992) 1182.

[15] GUDE, A., *Nucl. Fusion* **39** (1999) 127.

[16] ZOHM, H. et al., *Nucl. Fusion* **39** (1999) 577.

[17] GANTENBEIN, G. et al., *Phys. Rev. Lett.* **85** (2000) 1242.

[18] RYTER, F. et al., *This conference, paper No. IAEA-CN-77/EX2/2* (2000).

[19] YU, Q. et al., *Phys. Plasmas* **7** (2000) 312.